Inorg. Chem. **2006**, *45*, 4902–4909

Iron(III)–Nitro Porphyrins: Theoretical Exploration of a Unique Class of Reactive Molecules

Jeanet Conradie[†,‡] and Abhik Ghosh*[,†]

Department of Chemistry, University of Tromsø, N-9037 Tromsø, Norway, and Department of Chemistry, University of the Free State, 9300 Bloemfontein, South Africa

Received March 5, 2006

DFT(PW91/TZP) calculations, including full geometry optimizations, have been carried on $[Fe^{II}(P)(NO_2)]^-$, $Fe^{III}(P)(NO_2)$, $[Fe^{II}(P)(NO_2)(py)]^-$, $Fe^{III}(P)(NO_2)(py)$, $[Fe^{III}(P)(NO_2)_2]^-$, and $Fe^{III}(P)(NO_2)(NO)$, where P is the unsubstituted porphine dianion, as well as on certain picket fence porphyrin (TPivPP) analogues. The bonding in $[Fe^{II}(P)(NO_2)]^-$ and $Fe^{III}(P)(NO_2)$, as well as in their pyridine adducts, reveals a σ-donor interaction of the nitrite HOMO and the Fe d_{z^2} orbital, where the Fe–N_{nitro} axis is defined as the *z* direction and the nitrite plane is identified as *xz*. Both molecules also feature a π-acceptor interaction of the nitrite LUMO and the Fe d_{yz} orbital, whereas the SOMO of the Fe(III)–nitro complexes may be identified as d_{xz}. The Fe(III)–nitro porphyrins studied all exhibit extremely high adiabatic electron affinities, ranging from about 2.5 eV for $Fe^{III}(P)(NO_2)$ and $Fe^{III}(P)(NO_2)(py)$ to about 3.4 eV for their TPivPP analogues. Transition-state optimizations for oxygen-atom transfer from $Fe^{III}(P)(NO_2)$ and $Fe^{III}(P)(NO_2)(py)$ to dimethyl sulfide yielded activation energies of 0.45 and 0.77 eV, respectively, which is qualitatively consistent with the observed far greater stability of $Fe^{III}(TPivPP)(NO_2)(py)$ relative to $Fe^{III}(TPivPP)(NO_2)$. Addition of NO to yield $\{FeNO\}^6$ nitro–nitrosyl adducts such as $Fe(P)(NO_2)(NO)$ provides another mechanism whereby Fe(III)–nitro porphyrins can relieve their extreme electron affinities. In $Fe(P)(NO_2)(NO)$, the bonding involves substantial Fe–NO π-bonding, but the nitrite acts essentially as a simple σ-donor, which accounts for the relatively long Fe–N_{nitro} distance in this molecule.

1. Introduction

Although already of long-standing interest, transition metal−nitrite interactions have attracted renewed attention in recent months and years.[1,2] Nitrite is the substrate for the heme and copper-based nitrite reductases (NIR),[3,4] which reduce it to NO. Very recently, Murphy[5] and Hasnain[6] and their colleagues have crystallographically observed unique side-on CuNO intermediates for Cu NIR. The interaction of nitrite with deoxyhemoglobin, again a process of long-standing interest, has attracted renewed attention as a source of hypoxic vasodilation.[7−12] Against this exciting backdrop, we have undertaken this DFT study of Fe(III)−nitro porphyrins. A direct biological role for iron(III)−nitro intermediates is yet to be established. However, nitrite does catalyze the reductive nitrosylation of ferriheme proteins,[13,14] a process perhaps best known as the source of β-cys-93

* To whom correspondence should be addressed. E-mail: abhik@chem.uit.no.
† University of Tromsø.
‡ University of the Free State.

(1) Wyllie, G. R. A.; Scheidt, W. R. *Chem. Rev.* **2002**, *102*, 1067−1090.
(2) Ford, P. C.; Lorkovic, I. M. *Chem. Rev.* **2002**, *102*, 993−1018.
(3) Farmer, P. J.; Sulc, F. *J. Inorg. Biochem.* **2005**, *99*, 166−184.
(4) Ranghino, G.; Scorza, E.; Sjogren, T.; Williams, P. A.; Ricci, M.; Hajdu, J. *Biochemistry* **2000**, *39*, 10958−10966.
(5) Tocheva, E. I.; Rosell, F. I.; Mauk, A. G.; Murphy, M. E. P. *Science* **2004**, *304*, 867.
(6) Antonyuk, S. V.; Strange, R. W.; Sawers, G.; Eady, R. R.; Hasnain, S. S. *Proc. Natl. Acad. Sci. U.S.A.* **2005**, *102*, 12041.
(7) Huang, K. T.; Keszler, A.; Patel, N.; Patel, R. P.; Patel, R. P.; Gladwin, M. T.; Kim-Shapiro, D. B.; Hogg, N. *J. Biol. Chem.* **2005**, *280*, 31126−31131.
(8) Hunter, C. J.; Dejam, A.; Blood, A. B.; Shields, H.; Kim-Shapiro, D.; Machado, R. F.; Tarekegn, S.; Mulla, N.; Hopper, A. O.; Schechter, A. N.; Power, G. G.; Gladwin, M. T. *Nature Med.* **2004**, *10*, 1122−1127.
(9) Cosby, K.; Partovi, K. S.; Crawford, J. H.; Patel, R. P.; Reiter, C. D.; Martyr, S.; Yang, B. K.; Waclawiw, M. A.; Zalos, G.; Xu, X. L.; Huang, K. T.; Shields, H.; Kim-Shapiro, D. B.; Schechter, A. N.; Cannon, R. O.; Gladwin, M. T. *Nature Med.* **2003**, *9*, 1498−1505.
(10) Kim-Shapiro, D. B.; Gladwin, M. T.; Patel, R. P.; Hogg, N. *J. Inorg. Biochem.* **2005**, *99*, 237−246.
(11) Luchsinger, B. P.; Rich, E. N.; Yan, Y.; Williams, E. M.; Stamler, J. S.; Singel, D. J. *J. Inorg. Biochem.* **2005**, *99*, 912−921.
(12) Lim, M. D.; Lorkovic, I. M.; Ford, P. C. *J. Inorg. Biochem.* **2005**, *99*, 151−165.
(13) Fernandez, B. O.; Lorkovic, I. M.; Ford, P. C. *Inorg. Chem.* **2004**, *43*, 5393−5402.
(14) Ford, P. C.; Fernandez, B. O.; Lim, M. D. *Chem. Rev.* **2005**, *105*, 2439−2456.

10.1021/ic060362t CCC: $33.50
Published on Web 05/16/2006

S-nitrosohemoglobin (SNO−Hb),[15] although we do not know whether iron(III)−nitro intermediates are involved or not. We harbor the hope that eventually the electronic-structural insights obtained here will provide a broader context for biological metal−nitrite interactions.

Iron−nitro interactions are of considerable electronic-structural interest. As with many six-coordinate iron porphyrins, six-coordinate Fe(II) and Fe(III)−nitro porphyrins are low-spin species, $S = 0$ and $^1/_2$, respectively. More intriguingly, five-coordinate Fe−nitro porphyrins are also low-spin, which is rare for five-coordinate (5c) iron porphyrins.[16] Moreover, whereas Fe(II)−nitro porphyrins are relatively stable, Fe(III)−nitro species are reactive, readily transferring an oxygen atom (oxene) to suitable substrates to yield Fe(II)−NO or {FeNO}^{7} complexes.[1] Nevertheless, with the help of the picket fence porphyrin (TPivPP) ligand, the six-coordinate (6c) complex Fe^{III}(TPivPP)(NO_2)(py) has been synthesized and crystallographically characterized.[1] The corresponding presumptive 5c species Fe^{III}(TPivPP)(NO_2) has been detected only as an intermediate and characterized by EPR spectroscopy.[1] In addition, $S = ^1/_2$ Fe(III)−dinitro adducts such as the $[Fe^{III}(TPivPP)(NO_2)_2]^-$ anion and $S = 0$ {FeNO}^{6} nitro−nitrosyl adducts such as Fe^{III}(TPivPP)(NO_2)(NO) are relatively stable and have been crystallographically characterized.[1] In this study, we have carried out spin-unrestricted (gas-phase) DFT(PW91/TZP) calculations,[17,18] with full geometry optimization, on all these species as well as on their simplified porphine analogues. Below, we present our results on the optimized structures, bonding, and energetics of conceivable alternative spin states for all these species as well as on the transition states for oxygen-atom transfer from Fe^{III}(P)(NO_2) and Fe^{III}(P)(NO_2)(py) to dimethyl sulfide (DMS), which we have chosen as a prototypical oxene acceptor.

2. Basic Structural Trends

Figure 1 depicts highlights of the optimized geometries and Mulliken spin populations for 5c and 6c Fe(II)−,[16,19] Fe(III)−,[20,21] and Co(III)−nitro[22,23] porphyrins. As we discuss in more detail in Section 8, the key optimized geometry parameters are in reasonably good agreement with corresponding experimental values for analogous TPivPP derivatives. Figure 1 reveals some interesting structural trends: (1) The metal−N_{nitro}, N−O, and metal−$N_{porphyrin}$ distances are nearly identical for analogous (i.e., either 5c or 6c) Fe(II) and Fe(III) structures. (2) However, for a particular type of metal center, there are substantial structural differences between five- and six-coordinate metal−nitro complexes. Thus, for all three metal centers examined, the presence of a sixth pyridine ligand results in an elongation of the metal−N_{nitro} distance by roughly 0.07 Å, a trend that has also been experimentally observed, for example, from a comparison of $[Fe^{II}(TPivPP)(NO_2)]^-$ (1.849 Å) and $[Fe^{III}(TPivPP)(NO_2)(py)]^-$ (1.959 Å).[1] (3) Interesting variations in the metal−$N_{pyridine}$ distance can also be discerned for the three metal centers examined. For example, the Fe−$N_{pyridine}$ distance is distinctly longer for Fe(III) (2.17 Å) than for Fe(II) (2.09 Å) and Co(III) (2.11 Å); an examination of the MOs indicates that the nitro group's trans effect (i.e., the metal−$N_{pyridine}$ antibonding interaction) is considerably higher in the Fe(III) case. (4) Finally, the nitro groups do not exhibit a strong orientational preference vis-à-vis the porphyrin plane, exhibiting only a very mild (by <1 kcal/mol) preference for a staggered conformation relative to the metal−$N_{porphyrin}$ vectors.

3. Electronic Structure

A qualitative feel for the electronic structures of Fe(II)− and Fe(III)−nitro porphyrins is probably best conveyed via MO energy-level diagrams of the type shown in Figure 2. As a further aid in understanding, Figure 3 depicts the frontier MOs of the nitrite anion. Mulliken spin populations and spin density plots for Fe^{III}(P)(NO_2) and Fe^{III}(P)(NO_2)(py) are shown in Figure 1. As mentioned above, all the complexes studied are known or expected to be low-spin, which is also what we find in our calculations. For both $[Fe^{II}(P)(NO_2)]^-$ and Fe^{III}(P)(NO_2), the high-spin states were found to be about 1 eV higher in energy than the low-spin states. (The fact that we correctly reproduce the low-spin nature of the ground states is satisfying but not particularly impressive because most commonly used functionals, PW91 included, are somewhat biased in favor of low-spin transition-metal spin states,[24,25] although by considerably less than 1 eV.) What accounts for the low-spin states is that the nitrite anion, via its HOMO (Figure 3), is a strong σ-donor, whereas via its LUMO, it is a reasonably strong π-acceptor. For $[Fe^{II}(P)(NO_2)]^-$ (left, Figure 2), the σ-donor and π-acceptor interactions may be seen from the HOMO-5 and HOMO-2, respectively. If we define the metal−N_{nitro} vector as the *z* axis and the metal−N_{nitro} plane as the *xz* plane, then the singly occupied MO for the Fe(III) complexes may be regarded as essentially being a pure d_{xz} orbital (For the Cartesian coordinates of all molecules studied, see the Supporting Information). Compared to this electronic state ($^2B_1$ in the C_{2v} staggered conformation of Fe^{III}(P)(NO_2)), the alternative d_{yz}^1

(15) Luschinger, B. P.; Rich, E. N.; Gow, A. J.; Williams, E. M.; Stamler, J. S.; Singel, D. J. *Proc. Natl. Acad. Sci. U.S.A.* **2003**, *100*, 461−466.
(16) Nasri, H.; Wang, Y.; Huynh, B. H.; Scheidt, W. R. *J. Am. Chem. Soc.* **1991**, *113*, 717−719.
(17) All calculations were carried out using the ADF 2004 program system, the PW91 generalized gradient approximation (GGA) for both exchange and correlation, Slater-type TZP basis sets, tight criteria for SCF convergence and geometry optimization, and (unless otherwise mentioned) a spin-unrestricted formalism. For a description of the methods used, see: Velde, G. T.; Bickelhaupt, F. M.; Baerends, E. J.; Guerra, C. F.; Van Gisbergen, S. J. A.; Snijders, J. G.; Ziegler, T. *J. Comput. Chem.* **2001**, *22*, 2001.
(18) For a recent review of metalloporphyrin−NO bonding, see: Ghosh, A. *Acc. Chem. Res.* **2005**, *38*, 943−954.
(19) Nasri, H.; Ellison, M. K.; Krebs, C.; Huynh, B. H.; Scheidt, W. R. *J. Am. Chem. Soc.* **2000**, *122*, 10795−10804.
(20) Nasri, H.; Wang, Y.; Hanh, B. H.; Walker, F. A.; Scheidt, W. R. *Inorg. Chem.* **1991**, *30*, 1483−1489.
(21) Cheng, L.; Powell, D. R.; Khan, M. A.; Richter-Addo, G. B. *Chem. Commun.* **2000**, 2301−2302.
(22) Jene, P. G.; Ibers, J. A. *Inorg. Chem.* **2000**, *39*, 3823−3827.
(23) Goodwin, J.; Kurtikyan, T.; Standard, J.; Walsh, R.; Zheng, B.; Parmley, D.; Howard, J.; Green, S.; Mardyukov, A.; Przybyla, D. E. *Inorg. Chem.* **2005**, *44*, 2215−2223.
(24) Ghosh, A.; Taylor, P. R. *Curr. Opin. Chem. Biol.* **2003**, *7*, 113−124.
(25) Ghosh, A.; Taylor, P. R. *J. Chem. Theory Comput.* **2005**, *1*, 591−600.

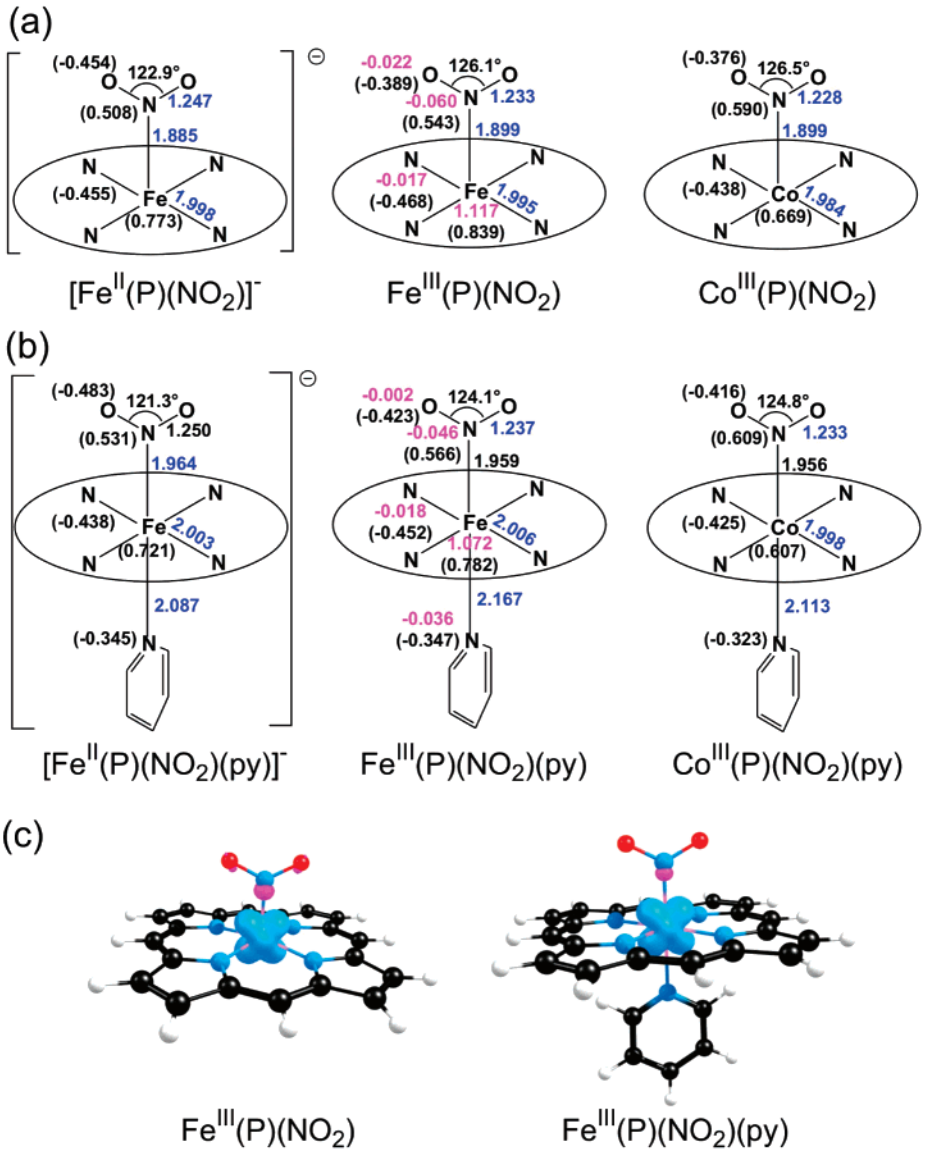

Figure 1. Selected PW91/TZP results: (a, b) distances (Å, blue), angles (deg, black), Mulliken charges (black), and spin populations (magenta); (c) spin density profiles.

($^2B_2$) or d_{xy}^1 ($^2A_1$) are 0.2 and 0.3 eV higher in energy, respectively.

Perhaps the most revealing calculated property of the Fe(III)−nitro complexes is the (adiabatic) electron affinity, which is 2.55 and 2.47 eV for $Fe^{III}(P)(NO_2)$ and $Fe^{III}(P)(NO_2)(py)$, respectively. By comparison, the electron affinities for typical metalloporphyrins (such as Ni(II) or Zn(II) porphyrins) are 1−1.5 eV. The enormous electron affinities provide a quantitative measure of the extremely electron-deficient character of the Fe(III) centers in these molecules, which will be a recurring theme in this study; as we will see in the remainder of the paper, iron(III)−nitro porphyrins try to relieve their "hunger" for electron density in a variety of ways.

4. Modeling Oxene Transfer from the Fe(III)−Nitro Unit

Whereas Fe(II)− and Co(III)−nitro porphyrins are relatively stable, Fe(III)−nitro porphyrins are unstable, readily transferring one of the nitro oxygens to oxygen-atom acceptors.[26] Indeed, evidence for the existence of a 5c Fe(III)−nitro porphyrin consists solely of EPR detection of a low-spin intermediate (with a rhombic EPR spectrum) in an oxygen-transfer reaction undergone by the Fe^{III}(TPivPP)$(NO_2)_2^-$ anion.[26] In contrast, a 5c Fe(II)−nitro TPivPP complex is not only stable in solution under anaerobic conditions but has also been crystallographically characterized.[16,19] Though quite reactive, the 6c complex Fe^{III}(TPivPP)(NO_2)(py) has also lent itself to a crystallographic analysis. In this study, we have optimized the transition states for oxene transfer from both 5c $Fe^{III}(P)(NO_2)$ and 6c $Fe^{III}(P)(NO_2)$(py) to the oxygen-atom acceptor dimethyl sulfide (DMS). Calculated energy profiles (as a function of the distance between the migrating oxygen and the DMS sulfur) are shown in Figure 4, whereas key geometrical parameters and spin density plots for the two transition states are shown in

(26) Munro, O. Q.; Scheidt, W. R. *Inorg. Chem.* **1998**, *37*, 2308−2316.

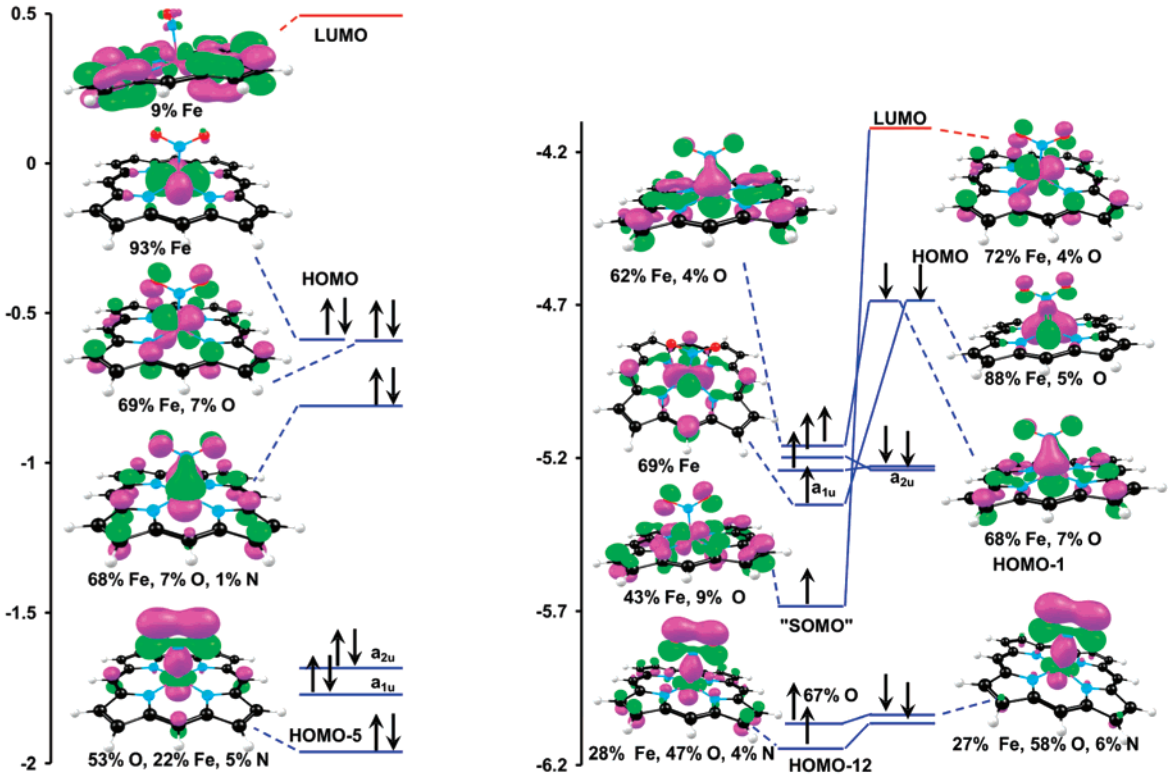

Figure 2. Frontier MO energy-level diagrams (eV) for $[Fe^{II}(P)(NO_2)]^-$ (left) and $Fe^{III}(P)(NO_2)$ (right). Note that spin-restricted calculations have been used for $[Fe^{II}(P)(NO_2)]^-$. Primarily porphyrin-based MOs are not graphically shown.

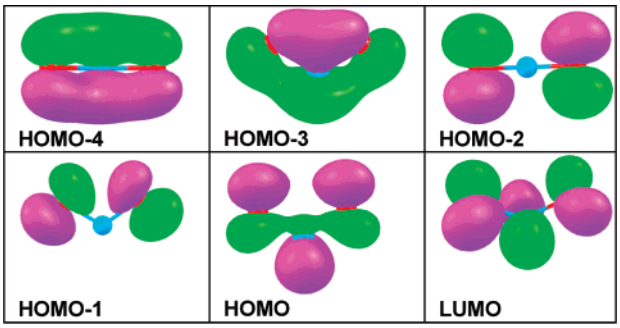

Figure 3. Nitrite frontier MOs.

Figure 5. Both transition states exhibited a single imaginary frequency.

Relative to the starting materials, the energies of the transition states (activation energies) are 0.45 eV for $Fe^{III}(P)(NO_2)$ and 0.77 eV for $Fe^{III}(P)(NO_2)(py)$. Qualitatively, these numerical results are satisfying. Both values are low, consistent with the reactive nature of Fe(III)−nitro complexes; moreover, the activation energy is substantially lower for 5c $Fe^{III}(P)(NO_2)$, again consistent with experimental trends for analogous TPivPP complexes.

The reaction profile may be described as follows. As the DMS sulfur approaches the migrating oxygen, the N−O bond involving that oxygen breaks (i.e., stretches) sharply, whereas the FeNO units in the transition states more or less take on the geometrical and electronic characteristics (as judged from the spin density profiles shown in Figure 5) of a typical $\{FeNO\}^7$ unit. Once the transition states are reached, the

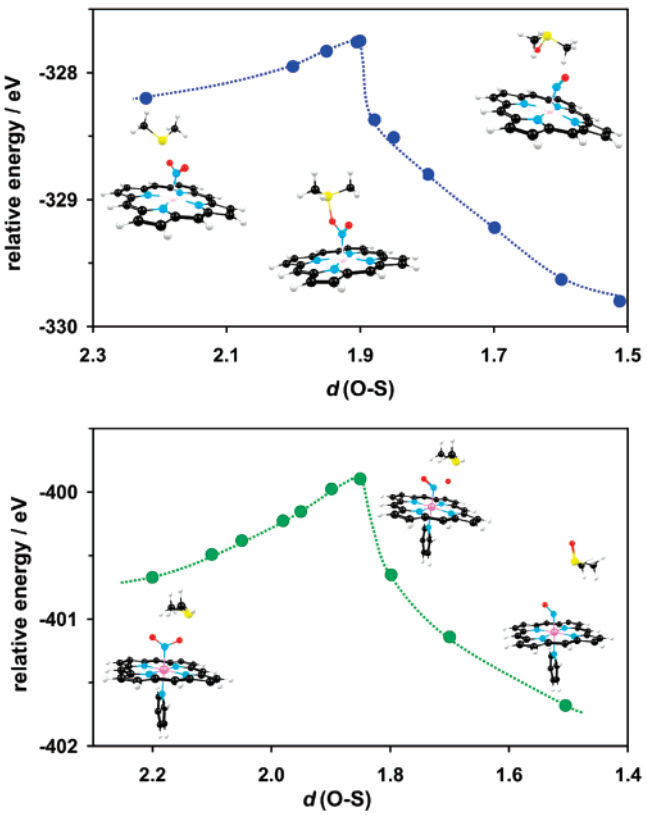

Figure 4. Energy profiles (eV) for the $Fe^{III}(P)(NO_2) + S(CH_3)_2$ (top) and (b) $Fe^{III}(P)(NO_2)(py) + S(CH_3)_2$ (bottom) reactions as a function of *d*(S,O) (Å), with all other internal coordinates being fully optimized. Note that the absolute values of the energies shown along the vertical axis are meaningless.

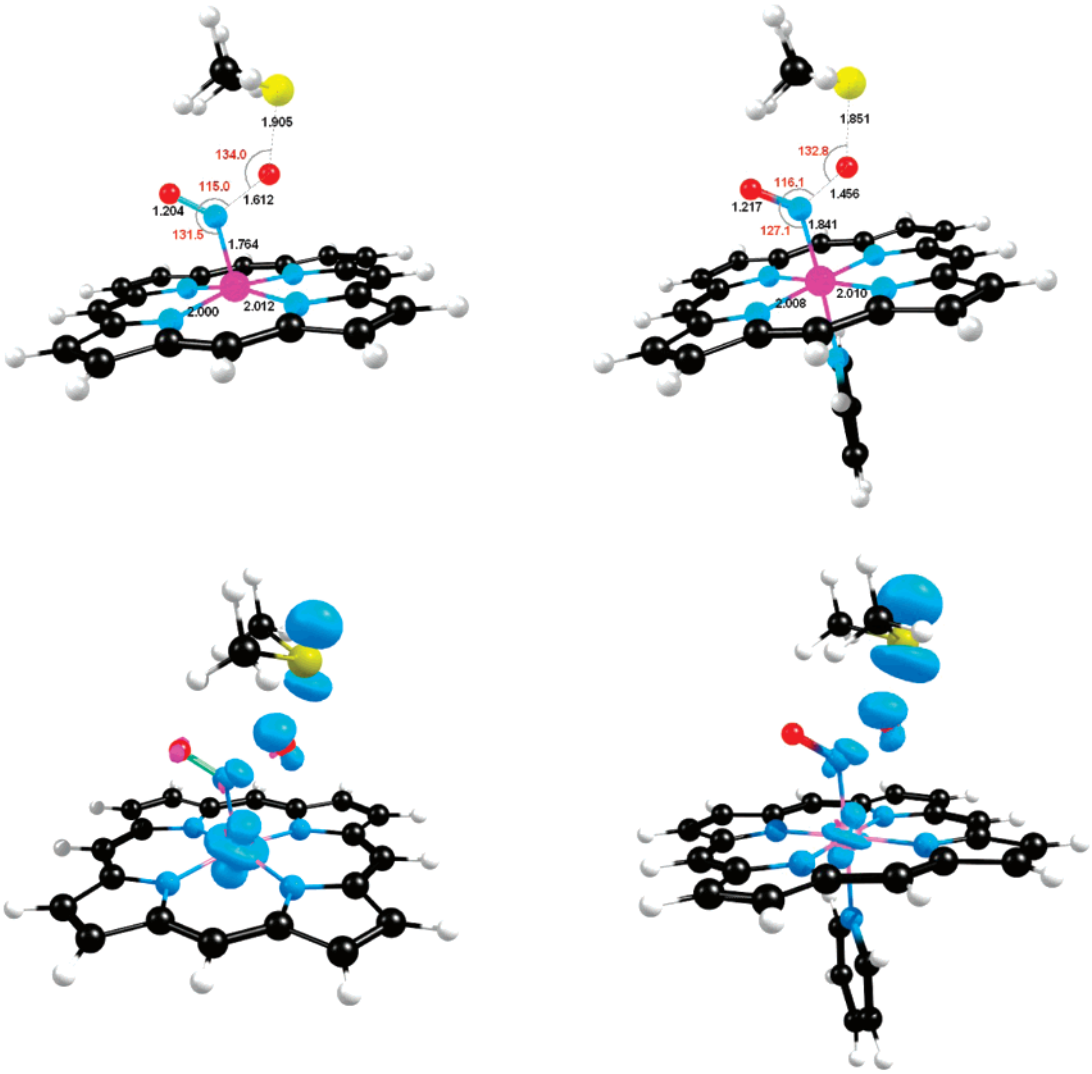

Figure 5. Structural highlights (Å, deg; top) and spin density profiles (bottom) for the transition states of the $Fe^{III}(P)(NO_2) + S(CH_3)_2$ (left, imag. frequency 684 cm^{-1}) and (b) $Fe^{III}(P)(NO_2)(py) + S(CH_3)_2$ (right, imag. frequency 492 cm^{-1}) reactions.

energy of the reactive system drops precipitously as the product dimethyl sulfoxide slides away.

5. Fe(III) *trans*-Dinitro Complexes

Iron(III) *trans*-dinitro complexes are moderately stable, and the TPivPP derivative has been crystallographically analyzed.[27−29] Nevertheless, these complexes too readily undergo oxene transfer under certain mild conditions. Figure 6 depicts highlights of the optimized geometries, Mulliken charges, and spin populations for $[Fe^{III}(P)(NO_2)_2]^-$ and $[Co^{III}(P)(NO_2)_2]^-$ as well as a spin density plot and frontier MO energy-level diagram for $[Fe^{III}(P)(NO_2)_2]^-$. The geometries of the two dinitro complexes are quite similar to each other, but both feature substantially longer metal−N_{nitro} distances than the corresponding mononitro species $Fe^{III}(P)(NO_2)$ and $Co^{III}(P)(NO_2)$ (Figure 1), respectively. For $[Fe^{III}(P)(NO_2)_2]^-$, a conformation in which the two nitro groups are coplanar is favored by 0.2 eV relative to a perpendicular conformation, whereas for $Co^{III}(P)(NO_2)$, the coplanar and perpendicular conformations are equienergetic.

The electronic configuration for the $[Fe^{III}(P)(NO_2)_2]^-$ anion may be described as d_{xz}^1, exactly as in the case of $Fe^{III}(P)(NO_2)$, and the spin density is essentially entirely on the iron. However, note that the Mulliken charge on the iron is considerably lower (+0.67) for $[Fe^{III}(P)(NO_2)_2]^-$ than for $Fe^{III}(P)(NO_2)$ (+0.84). This is qualitatively consistent with the much more subdued hunger for electron density and greater stability of the Fe(III)−dinitro complex relative to the 5c mononitro complex.

6. {FeNO}^{6} Nitro−Nitrosyl Complexes

In the presence of excess NO and traces of air (which also results in traces of NO_2 and N_2O_3), iron(II) porphyrins yield diamagnetic {FeNO}^{6} nitro−nitrosyl complexes, which

(27) Nasri, H.; Goodwin, J. A.; Scheidt, W. R. *Inorg. Chem.* **1990**, *29*, 181.
(28) Nasri, H.; Wang, Y.; Huynh, B. H.; Walker, F. A.; Scheidt, W. R. *Inorg. Chem.* **1991**, *30*, 1483−1489.
(29) Nasri, H.; Haller, K. J.; Wang, Y.; Huynh, B. H.; Scheidt, W. R. *Inorg. Chem.* **1992**, *31*, 3459−3467.

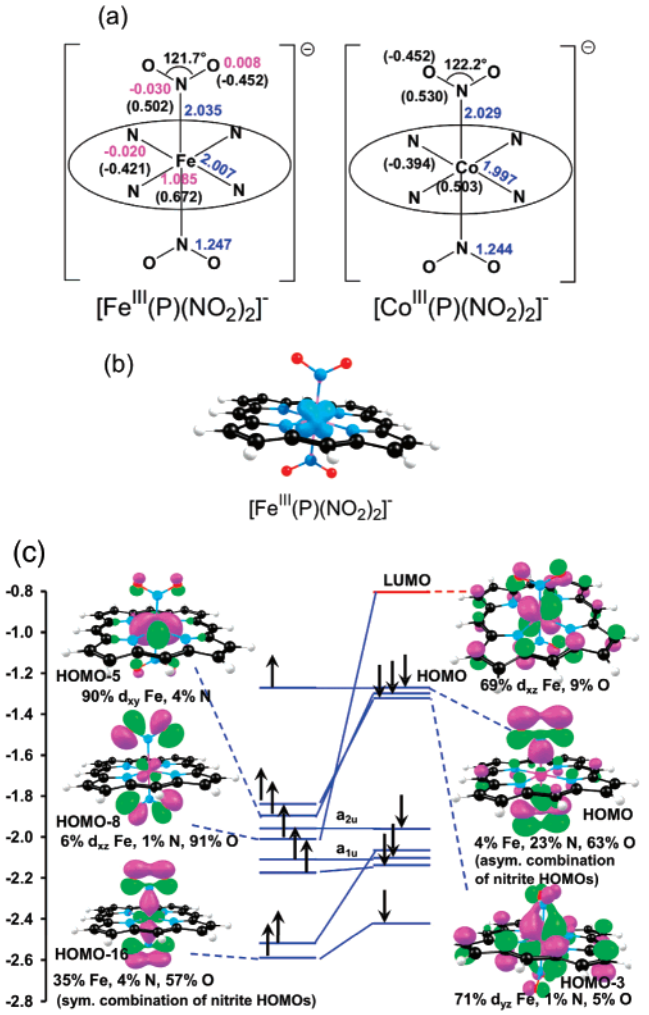

Figure 6. $[Fe(P)(NO_2)_2]^-$ and $[Co(P)(NO_2)_2]^-$: (a) selected distances (Å, blue), angles (deg, black), Mulliken charges (black), and spin populations (magenta); (b) spin density plot for $[Fe(P)(NO_2)_2]^-$; (c) frontier MO energy-level diagram for $[Fe(P)(NO_2)_2]^-$. Primarily porphyrin-based MOs are not graphically shown.

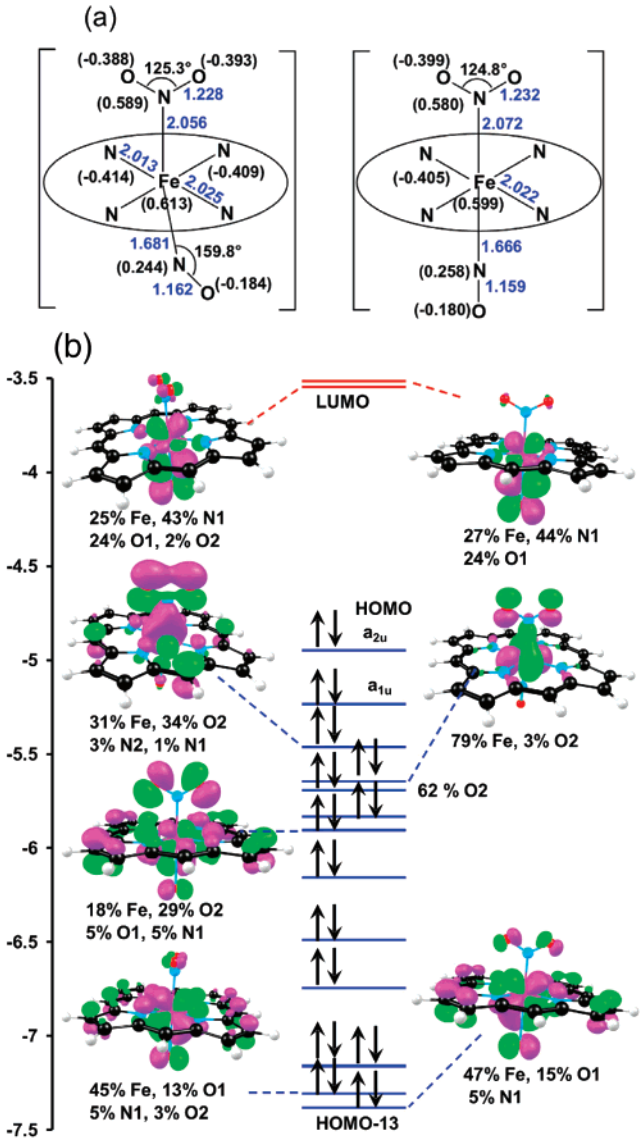

Figure 7. (a) Equienergetic C_s and C_{2v} optimized structures (Å, deg) and Mulliken charges of $Fe(P)(NO_2)(NO)$; (b) frontier MO energy-level diagram (eV) for the C_{2v} structure.

appear to be moderately stable and relatively common products in heme−NO_x chemistry.[30−32] Thus, several such complexes have been isolated and crystallographically characterized.[33,34]

Coppens, Richter-Addo, and their co-workers have also reported DFT calculations on $Fe^{III}(P)(NO_2)(NO)$, focusing on novel single- and double-linkage isomerism phenomena in this compound.[35] For the sake of completeness, we have repeated here some calculations on this species, and our results (which are consistent with the earlier findings[35]) are as follows. Figure 7 presents optimized geometries for C_{2v} and C_s symmetry constraints, Mulliken charges, and an MO energy-level diagram for $Fe^{III}(P)(NO_2)(NO)$ and some of the notable points are as follows.

A starting geometry with a strongly bent nitrosyl group resulted in an optimized geometry with an Fe−N_{NO}−O_{NO} angle of about 160° as well as an Fe−N_{NO} vector tilted in the same direction as the bending of the nitrosyl group. Remarkably but not altogether surprisingly, this tilted and bent geometry of $Fe^{III}(P)(NO_2)(NO)$ was found to have the same energy as the C_{2v} symmetry-constrained optimized structure, strongly suggesting a very soft potential for cooperative tilting and bending of the nitrosyl group. Such a potential-energy surface was first noted by Ghosh and Bocian[36,37] for carbonmonoxyhemes and was subsequently confirmed by many other laboratories.[38] Actually, the Ghosh−Bocian potential applies quite generally to a variety

(30) Lim, M. D.; Lorkovic, I. M.; Wedeking, K.; Zanella, A. W.; Works, C. F.; Massick, S. M.; Ford, P. C. *J. Am. Chem. Soc.* **2002**, *124*, 9737−943.
(31) Settin, M. F.; Fanning, J. C. *Inorg. Chem.* **1988**, *27*, 1431.
(32) Yoshimura, T. *Inorg. Chim. Acta* **1984**, *83*, 17
(33) Ellison, M. K.; Schulz, C. E.; Scheidt, W. R. *Inorg. Chem.* **1999**, *38*, 100−108.
(34) Nasri, H.; Ellison, M. K.; Shang, M.; Schulz, C. E.; Scheidt, W. R. *Inorg. Chem.* **2004**, *43*, 2932−2942.
(35) Lee, J.; Kovalevsky, A. Y.; Novozhilova, I. V.; Bagley, K. A.; Coppens, P.; Richter-Addo, G. B. *Inorg. Chem.* **2004**, *43*, 2932−2942.
(36) Ghosh, A.; Bocian, D. F. *J. Phys. Chem.* **1996**, *100*, 6363−6367.
(37) Vangberg, T.; Bocian, D. F.; Ghosh, A. *J. Biol. Inorg. Chem.* **1997**, *2*, 526−530.
(38) Spiro, T. G.; Kozlowski, P. M. *Acc. Chem. Res.* **2001**, *34*, 137−144.

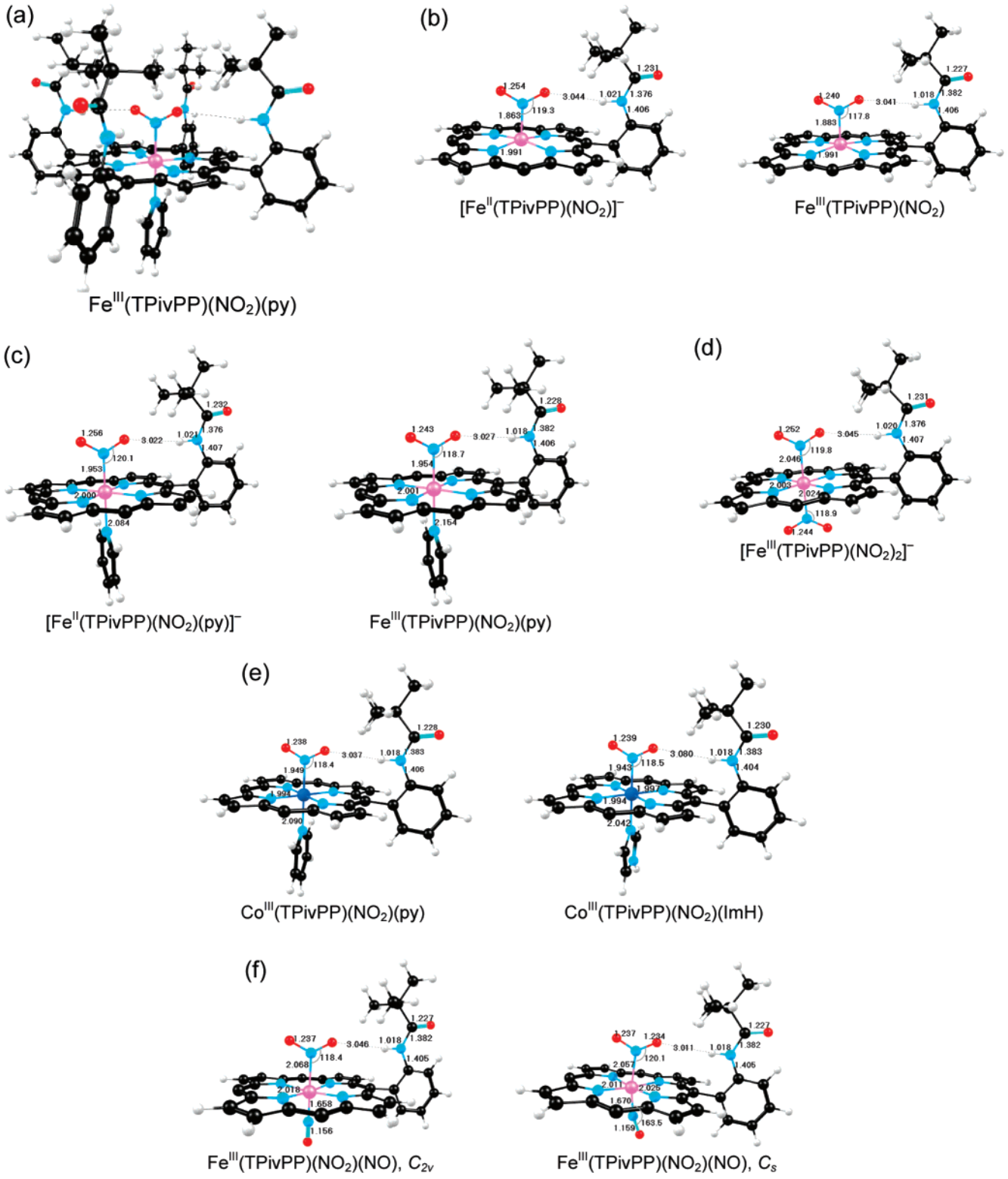

Figure 8. Highlights of the optimized structures for different TPivPP complexes. In the interest of clarity, except in part (a), only one pivalamidophenyl moiety is shown in each case.

of {MXO}^{6} complexes, including {FeNO}^{6} porphyrins and, more loosely, even to {FeNO}^{7} complexes.[39] Given the existence of a considerable body of literature on this topic,[36−39] we will refrain from discussing it again here, except to note that bent {FeNO}^{6} groups, though not common, have indeed been crystallographically observed. Thus, M^{III}(Por)(NO)Ar (M = Fe, Ru, and Os) complexes[40]

(39) Tangen, E.; Conradie, J.; Ghosh, A. *Inorg. Chem.* **2005**, *44*, 8699−8706.

(40) Richter-Addo, G. B.; Wheeler, R. A.; Hixson, C. A.; Chen, L.; Khan, M. A.; Ellison, M. K.; Schulz, C. E.; Scheidt, W. R. *J. Am. Chem. Soc.* **2001**, *123*, 6314−6326.

Table 1. Comparison of Selected Computed and Experimental Geometry Parameters (Å, deg) for Metal−Nitro Picket Fence Porphyrin Complexes[a]

compd	average M−N_{por}	average M−N_{NO_2}	average O−N_{NO_2}	M−L_{trans}[b]	O−N−O	ref
$[Fe^{II}(TPivPP)(NO_2)]^-$; $S = 0$	1.991 (**1.970**)	1.863 (**1.849**)	1.254 (**1.243**)		121.4 (**119.5**)	16,19
$[Fe^{II}(TPivPP)(NO_2)(py)^-$; $S = 0$	2.000 (**1.990**)	1.953 (**1.951**)	1.256 (**1.257**)	2.084 (**2.032**)	119.9 (**116.6**)	19
$Fe^{III}(TPivPP)(NO_2)(py)$; $S = 1/2$	2.001 (**1.983**)	1.954 (**1.960**)	1.243 (**1.233**)	2.154 (**2.093**)	122.5 (**119.9**)	28
$[Fe^{III}(TPivPP)(NO_2)_2]^-$; $S = 1/2$	2.003 (**1.992**)	2.046 (**2.001**)	1.252 (**1.233**)	2.025 (**1.969**)	120.3 (**118.8**,**119.8**)[c]	28
$Fe^{III}(TPivPP)(NO_2)(NO)$; $S = 0$; C_{2v}[d]	2.018 (**2.000**)	2.068 (**2.002**)	1.237 (**1.226**)	1.658 (**1.668**)	123.3 (**120.8**)	20
$Fe^{III}(TPivPP)(NO_2)(NO)$; $S = 0$; C_s[d]	2.018 (**1.996**)	2.057 (**1.998**)	1.235 (**1.223**)	1.670 (**1.671**)	123.6 (**121.4**)	20
$Co^{III}(TPivPP)(NO_2)(ImH)$; $S = 0$[e]	1.997 (**1.964**)	1.943 (**1.898**)	1.240 (**1.223**)	2.042 (**1.995**)	122.9 (**119.8**)	22

[a] Format: calcd (**expt**). [b] L_{trans} denotes the ligand trans to the nitro group on the picket fence side of the porphyrin. [c] There are wo different orientations in the crystal structure. [d] Two different molecular site symmetries are found in the crystal structure. [e] The compound studied experimentally was $Co^{III}(TpivPP)(NO_2)(1\text{-MeIm})$.

and an $\{FeNO\}^6$ nitrophorin 4 crystal structure[41] all exhibit MNO angles of around 160°.

With regard to the optimized structures, note the dramatic difference between the Fe−N_{nitro} and Fe−N_{NO} distances, the former exceeding the latter by nearly 0.4 Å, which is in fair agreement with what has been experimentally observed for $Fe(TPivPP)(NO_2)(NO)$.[33] Note that the Fe−N_{nitro} distance in $Fe(P)(NO_2)(NO)$ is also considerably longer, by roughly 0.1 Å, than that in any of the iron−nitro structures shown in Figure 1, whether Fe(II) or Fe(III), or 5c or 6c. The same trend has also been observed experimentally for analogous TPivPP complexes, and indeed, Scheidt and co-workers have commented at length on the highly variable nature of Fe^{II}−nitro π-bonding. The MO energy-level diagram for $Fe^{III}(P)(NO_2)(NO)$ shown in Figure 7 further illuminates this finding: as a π-acceptor, the NO completely outcompetes the nitro group; in the nitro−nitrosyl complexes, the nitro group acts as a simple σ-donor. Note also the rather low iron Mulliken charge for $Fe^{III}(P)(NO_2)(NO)$; it is lower than that for all the iron−nitro complexes that we have examined so far, which is consistent with the relatively subdued reactivity of the Fe(III) nitro-nitrosyls, compared with other Fe(III)−nitro species.

7. Effect of the Picket Fence

Last, we have carried out geometry optimizations for a number of Fe/Co−nitro picket fence porphyrin derivatives, which have also been crystallographically analyzed. Figure 8 presents highlights of these optimized geometries, whereas Table 1 presents a comparison of selected optimized and experimental geometry parameters. Our calculated results do not reveal any major differences in charge and spin density profiles between analogous porphine and picket fence porphyrin derivatives. Thus, the relative stability of the picket fence porphyrin derivatives must be attributed to the way the pivalamido groups hinder incoming electrophiles or other reactants. Both steric effects and O···H−N hydrogen-bonding interactions appear to minimize the reactivity of the coordinated nitrite ligands; however, in view of the large size of these molecules, we have not explicitly modeled the transition states for reactions involving picket fence porphyrin derivatives.

Table 1 shows that our calculations reproduce the majority of metal−ligand bond distances to within about 0.02−0.03 Å, tending to overestimate rather than underestimate these distances. However, certain distances are less well-reproduced. In particular, whereas the metal−N_{nitro} distances are generally well-reproduced in our calculations, metal−ligand distances involving axial ligands trans to the nitro group (as listed in the column "M−L_{trans}" in Table 1) appear to be significantly exaggerated in our calculations. However, the nitro−nitrosyl complex is an apparent exception to this generalization: here, the Fe−NO distance is well reproduced, whereas the Fe−N_{nitro} distance is significantly overestimated. These observations might suggest our calculations provide a somewhat imperfect description of trans effects. On the other hand, we do not know to what extent these discrepancies are attributable to crystal-packing effects that are not taken into account in our calculations. Additional calculations focusing more directly on the performance of different DFT functionals are underway in our laboratory and will be reported in due course.

8. Conclusions

In summary, we have carried out a first quantum chemical survey of iron(III)−nitro porphyrins, a class of intriguing and reactive molecules. Our specific conclusions are summarized in the Abstract and, as such, we will refrain from repeating them here. Very briefly, nitrite, as a ligand, is a reasonably strong σ-donor and a moderate π-acceptor, which explains the low-spin character of Fe(II)− and Fe(III)−nitro porphyrin species, which are five- or six-coordinate. In addition, our calculations provide some of the first numerical results quantifying the prodigiously electron-hungry nature of Fe(III)−nitro species, which relieve their electron affinities in a number of ways, most notably via oxygen-atom transfer from the nitro group, but also by forming dinitro and nitro−nitrosyl complexes.

Acknowledgment. This work was supported by the Research Council of Norway and the National Research Fund of the Republic of South Africa.

Supporting Information Available: Optimized Cartesian coordinates of all the molecules studied. This material is available free of charge via the Internet at http://pubs.acs.org.

IC060362T

(41) Roberts, S. A.; Weichsel, A.; Qiu, Y.; Shelnutt, J. A.; Walker, F. A.; Montfort, W. R. *Biochemistry* **2001**, *40*, 11327−11337.